

2023

Combined Effects of Fronts, Upwelling and the Biological Pump on Organophosphate Esters in the Changjiang (Yangtze) River Estuary During Summer

Jinghua Zhang

Follow this and additional works at: <https://digitalcommons.uri.edu/gsofacpubs>

The University of Rhode Island Faculty have made this article openly available.
Please let us know how Open Access to this research benefits you.

Terms of Use

This article is made available under the terms and conditions applicable towards Open Access Policy Articles, as set forth in our [Terms of Use](#).

Citation/Publisher Attribution

Zhang, J., Ma, Y., Zhong, Y., & Lohmann, R. (2023). Combined Effects of Fronts, Upwelling and the Biological Pump on Organophosphate Esters in the Changjiang (Yangtze) River Estuary During Summer. *JGR Oceans*, 128(12), e2023JC020081. <https://doi.org/10.1029/2023JC020081>
Available at: <https://doi.org/10.1029/2023JC020081>

This Article is brought to you for free and open access by the Graduate School of Oceanography at DigitalCommons@URI. It has been accepted for inclusion in Graduate School of Oceanography Faculty Publications by an authorized administrator of DigitalCommons@URI. For more information, please contact digitalcommons-group@uri.edu.

Combined Effects of Fronts, Upwelling and the Biological Pump on Organophosphate Esters in the Changjiang (Yangtze) River Estuary During Summer

The University of Rhode Island Faculty have made this article openly available.
[Please let us know](#) how Open Access to this research benefits you.

This is a pre-publication author manuscript of the final, published article.

Terms of Use

This article is made available under the terms and conditions applicable towards Open Access Policy Articles, as set forth in our [Terms of Use](#).

1 **Combined effects of fronts, upwelling and the biological pump on organophosphate**
2 **esters in the Changjiang (Yangtze) River estuary during summer**

3

4 Jinghua Zhang¹, Yuxin Ma^{1*}, Yisen Zhong^{1*}, Rainer Lohmann²

5

6 ¹School of Oceanography, Shanghai Jiao Tong University, 1954 Huashan Road, 200030

7 Shanghai, China

8 ²Graduate School of Oceanography, University of Rhode Island, 215 South Ferry Road,

9 Narragansett, 02882 Rhode Island, United States

10

11 Corresponding Author:

12 Yuxin Ma (yuxin.ma@sjtu.edu.cn)

13 Yisen Zhong (yisen.zhong@sjtu.edu.cn)

14

15 **Key Points**

16 Sediment inputs increased organophosphate ester concentrations in turbid bottom waters.

17 The biological pump strongly affected organophosphate esters in frontal/upwelling and
18 continental shelf regions.

19 Discharge from wastewater treatment plants contributed more than 50% of
20 organophosphate esters in the Changjiang River estuary.

21

22 **Abstract:**

23 Estuarine and coastal environments are important transport pathways and regional
24 sinks for anthropogenic pollutants. In this study, the occurrence and transport of the
25 continuously released organophosphate esters (OPEs) was investigated together with
26 physical and biochemical parameters throughout the water column in the Changjiang
27 (Yangtze) River estuary during the summer. Total dissolved and particulate OPEs showed
28 great spatial heterogeneity, with mean concentrations of 550 ± 280 ng/L in the estuary,
29 110 ± 270 ng/L in the front/upwelling zone, and 410 ± 450 ng/L in the continental shelf.
30 OPE concentrations in the estuarine bottom waters were high due to massive
31 terrestrial/sediment inputs. In contrast, the “surface enrichment and depth depletion” of
32 OPEs in the continental shelf was closely related to seasonal stratification. Reduced OPE
33 concentrations were observed in the frontal/upwelling zone due to isopycnal heaving.
34 Frontal activity and upwelling induced phytoplankton blooms in the coastal regions,
35 which jointly contributed to elevated OPEs beneath surface water with high
36 phytoplankton aggregation. The OPEs mainly originated from wastewater treatment plant
37 (WWTP) discharges, industrial pollution and consumer products. These OPEs generally

38 posed a low ecological risk to aquatic lives, but their long-term effects cannot be ignored
39 due to their continuous high production, usage and release.

40

41 **Plain Language Summary**

42 The environmental behavior and fate of anthropogenic contaminants, such as the
43 continuously released organophosphate esters (OPEs), is complex in estuaries and coastal
44 environments. In this study, the occurrence and transport of OPEs in the Changjiang
45 River estuary was associated with different oceanographic processes, including fronts,
46 upwelling and impacts of the biological pump. Dissolved and particulate OPEs varied
47 greatly from the estuary to the coastal region. High OPE concentrations were found in
48 turbid bottom waters of estuary, likely caused by massive sediment inputs. Due to
49 summertime stratification, the OPEs showed high levels in surface seawater, but
50 generally low concentrations in middle/bottom layers of the continental shelf. As for the
51 transition zone between the estuary and continental shelf where fronts/upwelling
52 coexisted, relatively low OPE concentrations were present through the water column,
53 because of the heaving of (cleaner) bottom water masses. Relatively higher OPE
54 concentrations were present just below the algae-rich surface water, probably caused by
55 the settling of biogenic particles with OPEs attached. The observed OPEs were mainly
56 from wastewater treatment plant (WWTP) discharges, industrial pollution and consumer
57 products. The ecological risks posed by OPEs to aquatic life cannot be ignored due to the
58 continuous exposure.

59

60 **Keywords:** organophosphate esters; Changjiang River estuary; frontal zone; upwelling

61 process; biological pump

62

63 **1. INTRODUCTION**

64 Organophosphate esters (OPEs) are a group of chemicals of emerging concern
65 (CECs) widely applied as flame retardants and plasticizers (Blum et al., 2019; Van der
66 Veen & de Boer, 2012). The market share of OPE flame retardants has considerably and
67 continuously increased, especially after the international regulation of the most
68 commonly used brominated flame retardants (BFRs), polybrominated diphenyl ethers
69 (PBDEs), in the early 2000s (Wang et al., 2020). The increasing consumption and broad
70 application of OPEs as additives have contributed to their high environmental mobility,
71 mainly via release to their surroundings by leaching, abrasion and volatilization (Gravel
72 et al., 2019). This has caused the global OPE distribution in a variety of environmental
73 compartments including air, seawater and sediment, generally with 2-3 orders of
74 magnitude higher concentrations than BFRs and other legacy Persistent Organic
75 Pollutants (POPs) (Cao et al., 2017; Li et al., 2017; Schmidt et al., 2019; Wolschke et al.,
76 2018). Moreover, some OPEs, such as tris (2-chloroethyl) phosphate (TCEP) and
77 triphenyl phosphate (TPhP), showed potential for carcinogenic and neurotoxic effects on
78 organisms (Olivero-Verbel et al., 2022). However, there is currently no international
79 regulation to address the increasing environmental pressure resulting from OPEs' usage
80 and emissions.

81 Due to the differences in the functional groups of OPEs, their physicochemical
82 properties, such as polarity, solubility and volatility, vary considerably. The
83 physicochemical properties affect the environmental behavior and fate of OPEs. For

84 example, chlorinated OPEs (Cl-OPEs) are considered persistent and mobile pollutants
85 due to their high water solubility and high recalcitrance to degradation (Rodgers et al.,
86 2018), and thus are generally difficult to remove in wastewater treatment plants (WWTPs)
87 (Zeng et al., 2015). Large quantities of Cl-OPEs are thus discharged into the aquatic
88 environment, and their distributions are further affected by hydrodynamic processes. In
89 contrast, some high molecular weight alkyl and aryl OPEs, with high octanol-water
90 partition coefficient ($\log K_{OW} > 5$), tend to be attached to particles (Fang et al., 2022).
91 These hydrophobic non-chlorinated OPEs (non-Cl-OPEs) therefore tend to
92 bioaccumulate in aquatic organisms and probably add additional stress to the ecosystem
93 (Wu et al., 2021).

94 Estuaries and continental shelves play a crucial role in the exchange of terrigenous
95 material between the land and open sea, and serve as important regional sinks for
96 anthropogenic pollutants (Chen et al., 2018; Gao et al., 2015). Several studies reported on
97 the occurrence of OPEs in the coastal environment (Fang et al., 2022; Pantelaki & Voutsas,
98 2021; Zhang et al., 2020), but only few described the influence of hydrological and/or
99 biogeochemical processes on the OPE transport in these regions (Zheng et al., 2022).
100 Hydrologically, riverine inflow carries large quantities of nutrients, terrigenous pollutants
101 and suspended sediments into estuaries and continental shelves (Chen et al., 2006; Gao et
102 al., 2015). Yet the fronts between oceanward freshwater and landward seawater are
103 considered transport barriers that restrict the spreading of the waterborne materials (Dong
104 et al., 2021). Many studies also revealed the impact of fronts on phytoplankton
105 aggregation and blooms (Li et al., 2022; Simpson et al., 1979). Notably, the coastal
106 upwellings bring nutrient-rich waters upward to the surface, facilitating the growth of

107 phytoplankton and other primary producers, and hence supporting fish stocks (Largier,
108 2020). Therefore, hydrodynamic processes not only regulate the physical transport of
109 (mobile) OPEs, but the coupled biogeochemical processes may also affect the
110 environmental behavior of OPEs. The OPEs with greater hydrophobicity typically exhibit
111 a propensity to bind to particles originating from both marine organisms and terrestrial
112 inputs, and then sink to deeper waters, primarily driven by the biological pump and
113 particulate settling (He et al., 2022). Understanding the impact of these coupled
114 hydrological-biogeochemical processes is essential for assessing the exposure risks of
115 biota to OPEs in the estuaries and coastal regions.

116 The Changjiang River (Yangtze) estuary receives large quantities of terrestrial
117 sediments, nutrients and organic pollutants discharged by WWTPs and non-point
118 atmospheric deposition sources located in the rapidly developing watershed (Liu et al.,
119 2007; Liu et al., 2019; Xu et al., 2018). The summer circulation off the estuary is shown
120 in Figure 1a, including the Changjiang Diluted Water (CDW) spreading toward the
121 northeast and the Taiwan Warm Current (TWC) originating from the Taiwan Strait (Hu &
122 Wang, 2016). The northeastward TWC passes through the coastal area, and may be
123 upwelled owing to the summer monsoon (Bai & Hu, 2004; Pei et al., 2009). The
124 coexistence of river plume and upwelling complicates the ecosystem dynamics in the
125 Changjiang River estuary. Using the physical, biogeochemical, dissolved and particulate
126 OPEs measurements, this research aims to (i) investigate the occurrence and possible
127 sources of dissolved and particulate OPEs; (ii) describe their hydrological and
128 biogeochemical processes; (iii) estimate the daily mass input of dissolved and particulate
129 OPEs, and (iv) assess the potential ecological risks posed by OPEs.

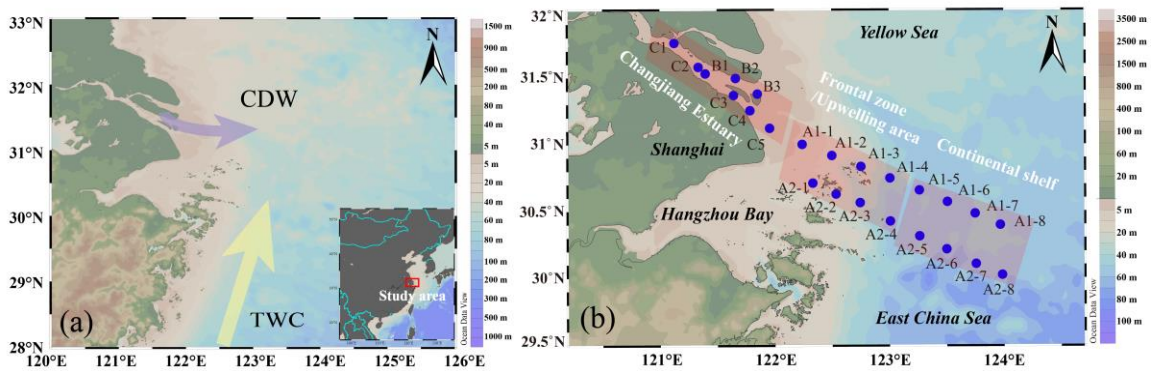
130

131 **2. MATERIALS AND METHODS**

132 **2.1 Sampling**

133 Sixty-one water samples, including both surface and subsurface waters, were
 134 collected from the Changjiang River estuary and its adjacent coastal waters of the East
 135 China Sea (ECS) on board research vessel *Zheyuke2* in July 2021 (Figure 1b). The
 136 sampling area can generally be divided into the estuary (B-C transects), the
 137 frontal/upwelling zone (sites A1-1~A1-4 & A2-1~A2-4), and the continental shelf area
 138 (sites A1-5~A1-8 & A2-5~A2-8). Approximate 1 L seawater was collected by Niskin
 139 bottles mounted on a conductivity-temperature-depth (CTD, SBE 911, Sea-Bird Co.)
 140 rosette at multiple depth levels. The samples were immediately filtered through a
 141 Whatman glass fiber filter (GF/F, 47 mm, 0.7 μm) to trap suspended particulate matter
 142 (SPM). The filtrates were then transferred into amber glass bottles and stored in a 4 °C
 143 refrigerator, while the filters were wrapped in aluminum foil and stored at -20 °C until
 144 pretreatment. The detailed sampling information is listed in Table S1.

145



146 Figure 1. The schematic circulation pattern in the Changjiang River estuary: (a) Changjiang Diluted
 147 Water (CDW), Taiwan Warm Current (TWC); (b) The sampling sites in the Changjiang River estuary
 148 and its adjacent area.

149 **2.2 Sample Analysis**

150 The extraction and purification of filtrates were conducted following the procedures
151 detailed prior with minor modifications (Quintana et al., 2008). The water samples were
152 spiked with 100 ng surrogates including d₁₂-tris-(2-chloroethyl) phosphate (d₁₂-TCEP),
153 d₁₅-triphenyl phosphate (d₁₅-TPhP) and d₂₇-tri-butyl phosphate (d₂₇-TnBP), and extracted
154 by liquid-liquid method with 50 mL dichloromethane (DCM) three times. Colored
155 extracts were further purified through a self-packed silica gel column (2 g anhydrous
156 sodium sulfate loaded onto 5 g silica gel) and eluted with 20 mL DCM/acetone (v:v =
157 1:1). Transparent extracts were passed directly through an anhydrous sodium sulfate
158 column to remove water. The treatments of SPM samples were modified from Wang et al.
159 (2018), as described in Text S1. The GF/F filter samples, with 100 ng surrogates added
160 overnight for equilibrium, were ultrasonically extracted with acetonitrile three times, then
161 the extracts were concentrated and purified on an Oasis Prime HLB (500 mg, 6 mL,
162 Waters, USA), and subsequently eluted with 8 mL hexane, 8 mL hexane/ethyl acetate
163 (v:v = 1:1) and 8 mL ethyl acetate. For both filtrate and GF/F, the samples were finally
164 concentrated and solvent-exchanged to hexane, with 100 ng p-terphenyl-d₁₄ spiked as
165 internal standard before instrumental analysis. The SPM concentrations on GF/F were
166 measured as the difference of pre- and post-filtration weighing (Table S1). The analyses
167 of other physical and biochemical parameters, including temperature, salinity, turbidity,
168 photosynthetically active radiation (PAR), dissolved oxygen (DO), chlorophyll *a* (Chl *a*)
169 and nutrients in water are described in Text S2.

170 **2.3 Reagents and Standards**

171 Twelve OPEs were analyzed including three Cl-OPEs (tris-(2-chloroethyl)

172 phosphate (TCEP), tris-(1-chloro-2-propyl) phosphate (TCPPs), tris-(1,3-dichloro-2-
173 propyl) phosphate (TDCP)), seven alkyl-OPEs (triethyl phosphate (TEP), tri-iso-propyl
174 phosphate (TiPrP), tri-propyl phosphate (TPrP), tri-iso-butyl phosphate (TiBP), tri-butyl
175 phosphate (TnBP), tri-pentyl phosphate (TPeP), tris-(2-ethylhexyl) phosphate (TEHP))
176 and two aryl-OPEs (triphenyl phosphate (TPhP) and 2-ethylhexyl diphenyl phosphate
177 (EHDPP)). All standards were purchased from AccuStandard (USA), except that TiPrP
178 was obtained from Chiron (Norway) and EHDPP from Dr. Ehrenstorfer (Germany).
179 Detailed physicochemical properties of OPEs are listed in Table S2. The targets were
180 analyzed using a gas chromatograph coupled to a triple quadrupole mass spectrometer
181 (GC-MS/MS, Agilent 7890B-7000D) equipped with a programmed temperature
182 vaporizer (PTV) injector. The details for the GC-MS/MS method are given in Text S3 and
183 Table S3. HPLC grade DCM, n-hexane, ethyl acetate and acetone were purchased from
184 Fisher Scientific Co (USA). Guaranteed reagent anhydrous sodium sulfate and
185 chromatographic silica gel (100-200 mesh) were supplied by Sinopharm Chemical
186 Reagent Co., Ltd. (China).

187 **2.4 Quality Assurance/Quality Control (QA/QC)**

188 For QA/QC, all amber glass bottles, GF/F filters and aluminum foil were preheated
189 at 500 °C for 5 h before use. The background values of OPEs in Niskin bottles and field
190 blanks with Milli-Q water were below the method detection limits (MDL). To assess
191 laboratory background contamination and analytical methods, one procedural blank and
192 one spiked blank (Milli-Q and blank filter) were included for each batch of ten samples,
193 during the pretreatment of seawater and filter samples (Table S4). The recoveries of
194 surrogates were 104% ± 14% for d₁₂-TCEP, 88% ± 26% for d₁₅-TPhP, 66% ± 17% for

195 d₂₇-TnBP in dissolved water samples and 90% ± 21% for d₁₂-TCEP, 107% ± 16% for d₁₅-
196 TPhP, 65% ± 6% for d₂₇-TnBP in SPM samples. The instrumental limit of detection
197 (LOD, defined as 3 times signal-to-noise ratio (S/N)) and quantification (LOQ, defined as
198 10 times S/N) for OPEs were in the range of 0.004-1.4 ng/L and 0.015-4.7 ng/L,
199 respectively. The MDL, calculated as the mean plus three times the standard deviation
200 (SD) of blanks, were 0.34 to 5.2 ng/L for dissolved OPEs and 0.054-1.5 ng/L for
201 particulate OPEs in seawater (Table S4).

202 **2.5 Data Analysis.**

203 For each sample, OPE concentrations were MDL corrected and blank subtracted.
204 The statistical analysis and principal component analysis-multiple linear regression
205 (PCA-MLR) were performed using SPSS 24.0; EHDPP was removed from the data
206 analysis with a detection frequency lower than 60% (Text S4). The redundancy analysis
207 (RDA) was performed using the R package ‘vegan’ to evaluate the importance of
208 physical and ecological factors to explain the variability of OPE concentrations in
209 seawater. Before the RDA analysis, the OPE concentrations were standardized to reduce
210 the influence of abundant compounds on the results of the ordination. To check for
211 multicollinearity between explanatory variables, variance inflation factor (VIF) was set to
212 VIF<10. The permutation tests were performed to confirm the significance of RDA
213 models and explanatory factors (Monte-Carlo, 999 permutations, significance level of $p \leq$
214 0.05). The concentration of OPEs for PCA-MLR and RDA was expressed as the sum of
215 the dissolved and particulate phases. For figures, the profile of physical/biogeochemical
216 variables and OPE concentrations were produced by Ocean Data View 5.5.2; Boxplots,
217 PCA and RDA statistical analysis, and results of ecological risk assessment were

218 visualized by Origin 2021.

219 **2.6 Mass Inflow Calculation**

220 The mass inflow of OPEs from Changjiang River (F , kg/d) was calculated as:

$$221 \quad F = C_i \times Q \times 10^{-9}$$

222 where C_i is the mean of total OPE concentrations in dissolved and particulate phase,
223 respectively (ng/L), calculated by trapezoidal integration of OPE concentrations through
224 the estuarine water column; and Q is the daily runoff of Changjiang River in July, 2021
225 (monthly runoff divided by the number of days, 117.8 billion m³/month,
226 <http://www.cjw.gov.cn/zwzc/bmgb/kzdmb/>).

227 **2.7 Risk Assessment**

228 A risk quotient (RQ) was calculated to assess the ecological risk of the observed
229 OPEs in surface water of the Changjiang River estuary:

$$230 \quad RQ = \frac{MEC}{PNEC} = \frac{MEC}{(LC_{50} \text{ or } EC_{50})/f}$$

231 where MEC is the measured environmental concentration of OPEs; LC_{50}/EC_{50} refers
232 to the 50% lethal/effect concentration obtained from acute toxicity tests on algae,
233 crustaceans and fish (Verbruggen et al., 2005). $PNEC$ is the predicted no-effect
234 concentration based on LC_{50}/EC_{50} . An assessment factor (f) of 1000 was used to interpret
235 the results inferred from intra- and interspecies susceptibility variability (Shi et al., 2020).
236 The biological risks were categorized as no significant impact ($RQ < 0.01$), low ($0.01 <$
237 $RQ < 0.1$), medium ($0.1 < RQ < 1.0$) and high ($RQ > 1.0$).

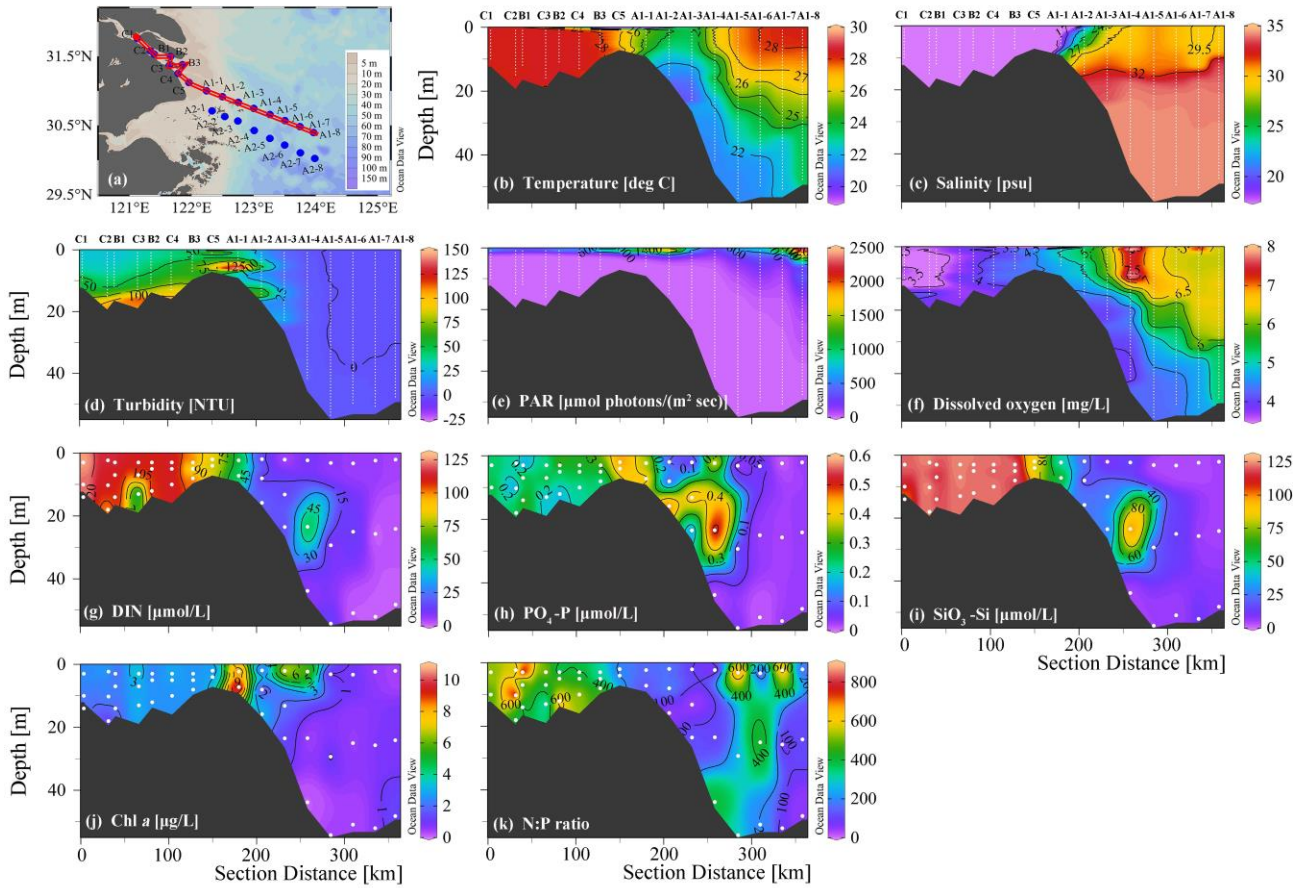
238

239 **3. RESULTS**

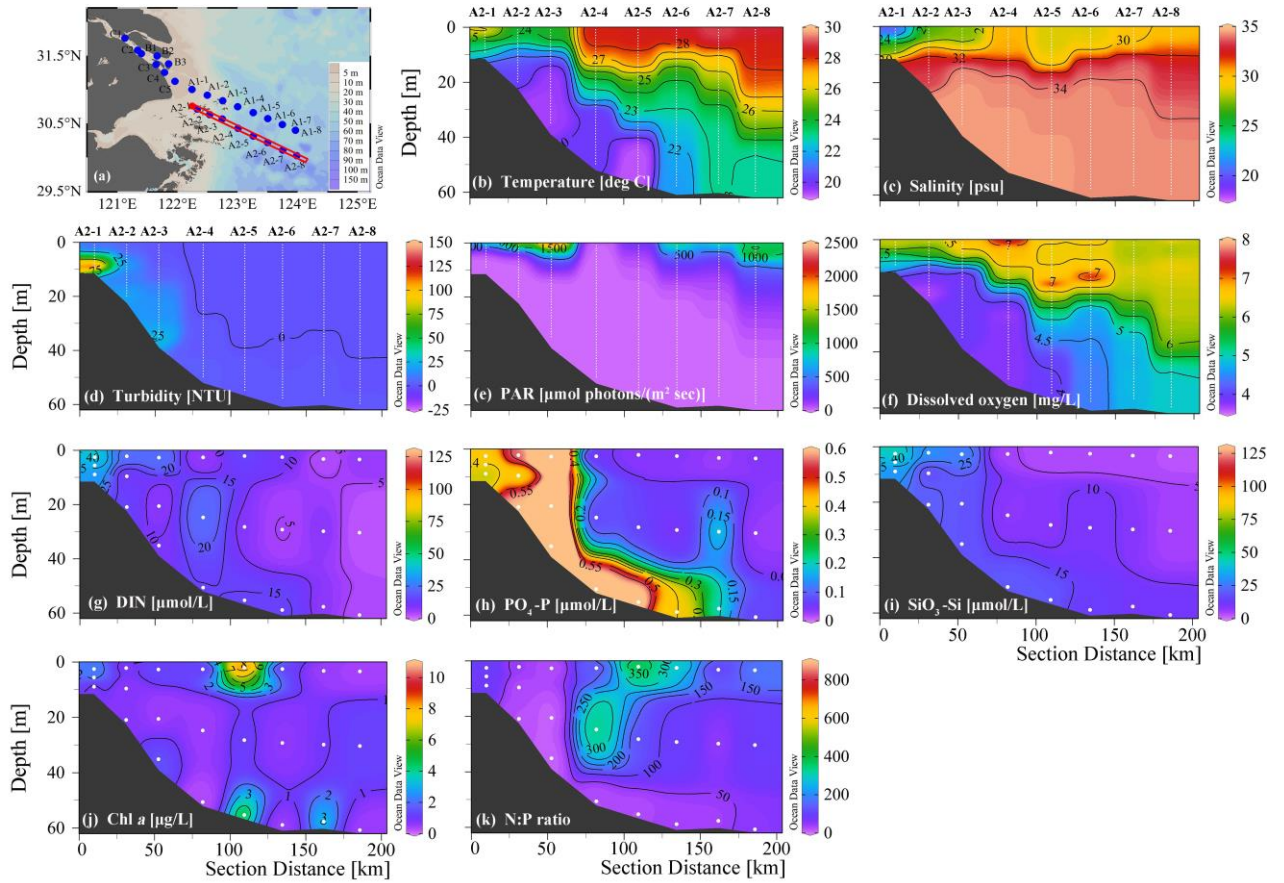
240 **3.1 Physical and biogeochemical characteristics**

241 As a typical land-ocean transition zone, the Changjiang River estuary and its
242 adjacent coastal waters showed great spatial heterogeneity in physical and biochemical
243 properties (Figure 2 & 3). In summer, the well-mixed estuarine water displayed high
244 temperature (mean: 28 °C), extremely low salinity (mean: 0.14 psu) and low DO (3.7
245 mg/L). On the continental shelf, the water column was stratified with the thermocline and
246 halocline of less than 10 m depth, and the surface water was characterized by comparably
247 higher temperature (> 28 °C), salinity (< 30 psu) and DO (> 6.2 mg/L) than the estuary
248 (Figure 2b, 2c, 2f & 3b, 3c, 3f). Moreover, the doming of temperature, salinity and DO
249 isolines was associated with elevated dissolved inorganic nitrogen (DIN, the sum of NO₃-
250 N, NH₄-N and NO₂-N), phosphate (PO₄-P) and silicate (SiO₃-Si) (Figure 2g, 2h, 2i & 3g,
251 3h, 3i), which indicated the summer upwelling of the TWC bottom waters along the slope
252 of submerged river valley beneath the surface frontal zone (Pei et al., 2009). The DIN and
253 SiO₃-Si concentrations declined sharply in the frontal zone along the transect B-C-A1 and
254 A2, whereas the PO₄-P concentrations peaked at the center of upwelling region, owing to
255 the bottom supply of nutrients-rich waters, as well as the transport barrier effect of the
256 fronts. High Chl *a* spots were found in the surface water of frontal/upwelling region (A1-
257 1~A1-4) and nearby (A2-5) (Figure 2j & 3j). This could be attributed to the upwelling of
258 rich nutrients to the surface layer that alleviates the potential PO₄-P limitation on one
259 hand (Figure 2k & 3k), and on the other hand the rapid decrease of turbidity from the
260 estuary (23-123 NTU) to the frontal/upwelling zone (almost 0 NTU, Figure 2d & 3d) that
261 dramatically enhances the light penetration and photosynthetically active radiation (PAR,

262 Figure 2e & 3e). In addition to the light and nutrients availability, the physical
 263 convergence at the frontal zone may have also contributed to these high Chl *a*
 264 concentrations (Li et al., 2022).



265
 266 Figure 2. The vertical profiles of temperature (b), salinity (c), turbidity (d), PAR (e), dissolved oxygen
 267 (f), nutrients (g-i) and Chl *a* (j), N:P ratio (k) in section B-C-A1 (a). White dash lines at each station
 268 represent CTD sensor data, and white points represent the laboratory measurement data



269

270 Figure 3. The vertical profiles of temperature (b), salinity (c), turbidity (d), PAR (e), dissolved oxygen
 271 (f), nutrients (g-i) and Chl *a* (j), N:P ratio (k) in section A2 (a). White dash lines at each station
 272 represent CTD sensor data, and white points represent the laboratory measured data

273

274 3.2 Occurrence and distribution of OPEs in seawater of Changjiang River estuary

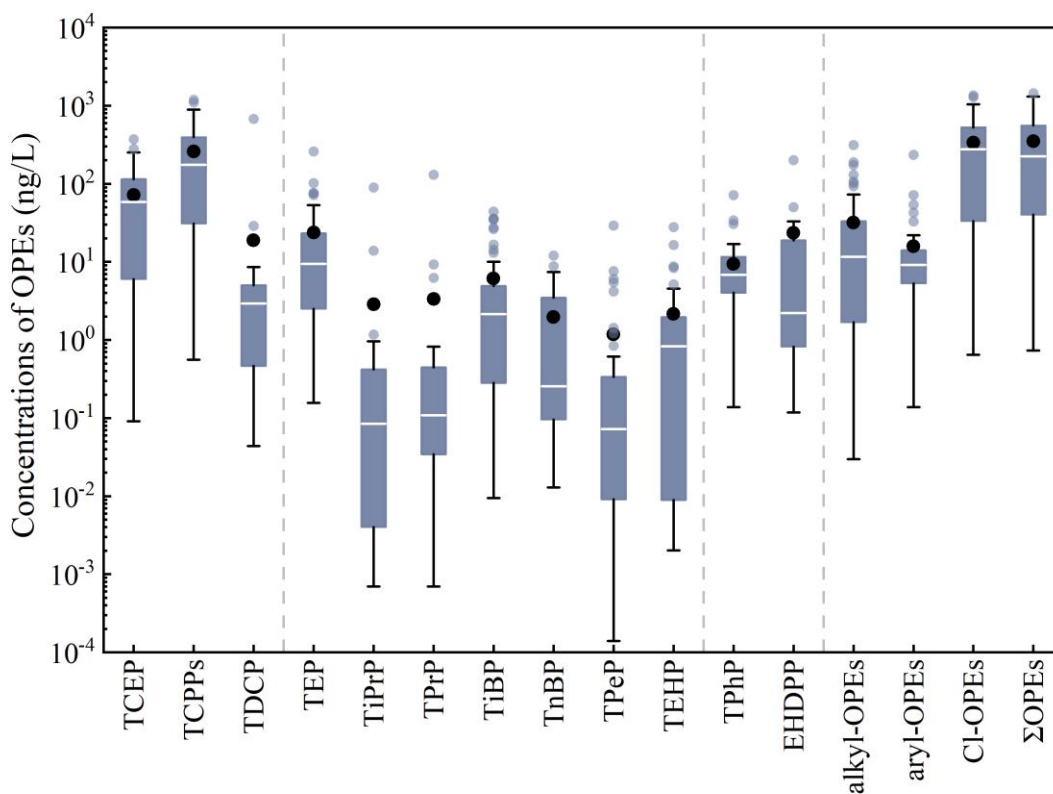
275 The detection frequencies of twelve individual OPEs ranged from 25%-90% (Table
 276 S5). Except for EHDPP (25%), both Cl-OPEs (> 70%) and non-Cl-OPEs (> 60%)
 277 displayed high detection frequencies. The total OPE concentrations (dissolved +
 278 particulate, Σ_{12} OPEs) throughout the water column ranged from 0.73 to 1400 ng/L, with a
 279 mean and median of 350 ± 380 ng/L and 220 ng/L, respectively (Figure 4). Three Cl-
 280 OPEs dominated the composition profile with a mean contribution of $70 \pm 28\%$, while

281 alkyl-OPEs and aryl-OPEs contributed $16 \pm 25\%$ and $14 \pm 19\%$ respectively. The major
282 compounds were TCPPs (260 ± 290 ng/L) and TCEP (72 ± 79 ng/L), followed by TEP
283 (24 ± 42 ng/L) and EHDPP (24 ± 49 ng/L). The dominance of Cl-OPEs, especially
284 TCPPs, in seawater was consistent with the recent measurements in the Bohai Bay and
285 Laizhou Bay (Chen et al., 2019; Lian et al., 2021), and of atmospheric OPEs (gaseous
286 and aerosol phase) in coastal regions (Castro-Jiménez et al., 2014; Li et al., 2018; Ma et
287 al., 2022), suggesting the importance of atmospheric sources. Detailed information of
288 individual OPE concentrations is given in Tables S6-S8.

289 A large proportion ($89 \pm 12\%$) of Σ_{12} OPEs was in the dissolved phase (Figure S1),
290 consistent with other studies in the aquatic environment (Pantelaki & Voutsas, 2021; Wang
291 et al., 2018). Notably, despite the low concentrations of particulate OPEs, the detection
292 frequencies of most individual OPE in particles exceeded 50%, except for EHDPP (15%).
293 Two compounds, TCPPs (4.8 ± 6.4 ng/L) and TPhP (6.9 ± 4.5 ng/L), showed relatively
294 higher abundance in the particulate phase (Table S5). The water-particle partitioning
295 exhibited higher particulate fractions for TPhP and TEHP, with mean contributions of 93%
296 and 50% respectively, followed by TDCP, TEP, TiPrP and TPeP with a mean of 33%-42%,
297 while the average particulate fraction of TCPPs, TCEP, TPrP, TiBP and TnBP was only
298 6%-28% (Figure S2a). These results agreed with those observed in other coastal regions,
299 such as northern Greece and San Francisco Bay (Pantelaki & Voutsas, 2021; Shimabuku et
300 al., 2022).

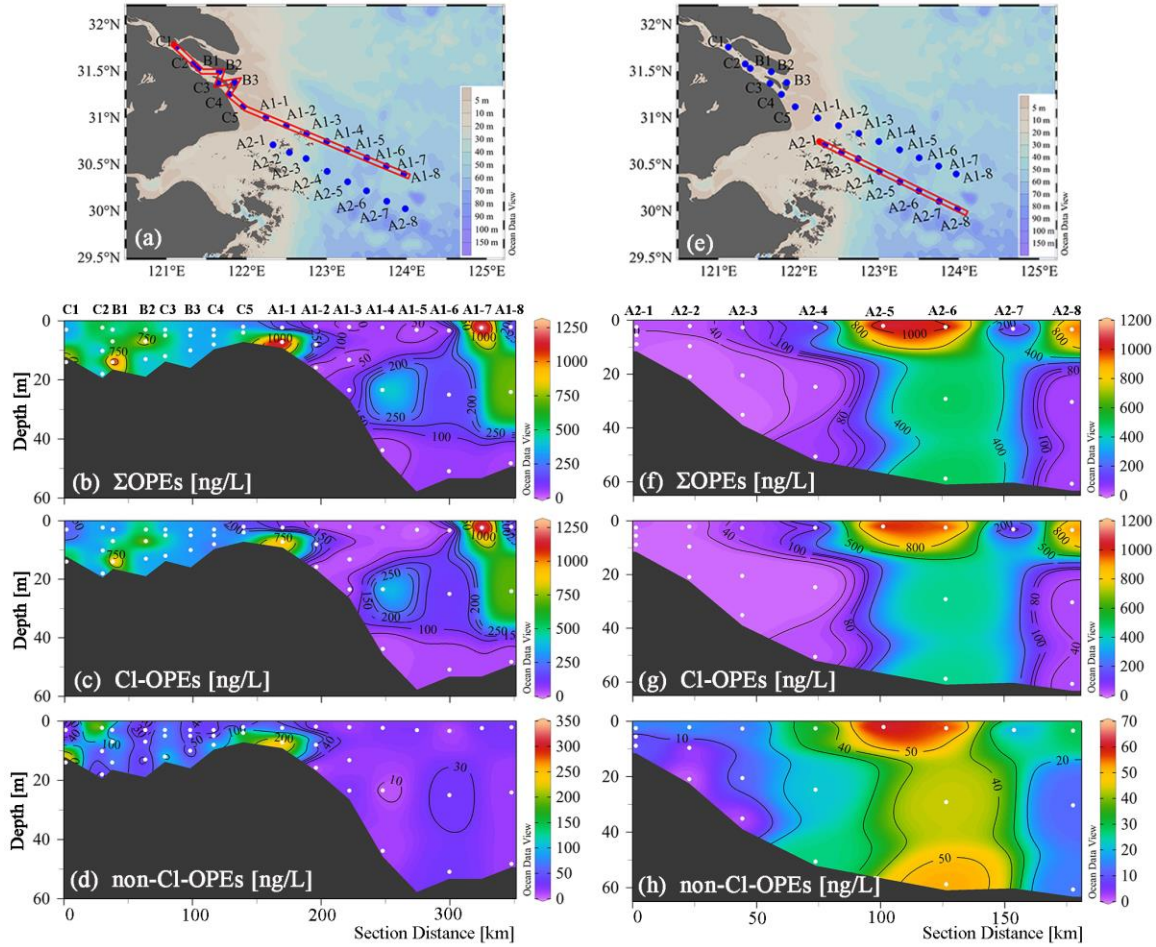
301 The water-particle partitioning coefficient (K_P , L/kg) has been widely used to
302 evaluate the partition behavior of OPEs in the aquatic environment (detailed calculation
303 method in Text S5) (Pantelaki & Voutsas, 2021). The logarithm of K_P for individual OPEs

304 ranged from 0.06-5.0 in seawater, and a significantly positive correlation was observed
 305 between $\log K_P$ and $\log K_{OW}$ (Figure S2b), indicating the water-particle partitioning of
 306 OPEs was influenced by hydrophobic interactions. It is noteworthy that the observed K_P
 307 values were generally lower than the theoretical K_{OW} , since the field measurements not
 308 only included contaminants that were truly dissolved, but also colloidal and/or associated
 309 with particles less than 0.7 μm .



310
 311 Figure 4. The statistical results of total (dissolved and particulate) OPE concentrations (ng/L) in (n =
 312 61) of the Changjiang River estuary. The white horizontal line inside each box represents the median
 313 based on measured concentrations; the black solid circles represent the mean concentrations of OPEs;
 314 the small size circles represent outliers; the boxes represent the 25th and 75th percentiles of
 315 concentrations above MDL and the black vertical lines mark the 95% confidence interval; the gray
 316 vertical dashed lines are to distinguish the statistical results of Cl-, alkyl-, and aryl- individual OPE

317 Σ_{12} OPEs displayed great spatial variability in our study area (Figure S3, Figure 5).
318 Relatively higher OPE concentrations were found throughout the estuarine water column
319 (B-C transects), with some highest concentrations occurring in bottom waters. The high
320 OPE concentrations coincided exactly with regions of high turbidity. In contrast, the
321 OPEs generally showed a ‘surface enrichment and depth depletion’ pattern in both
322 transects of the continental shelf area (sites A1-5~A1-8 & A2-5~A2-8). It is noteworthy
323 that the inputs of OPEs from Changjiang River seemed to be interrupted in the
324 frontal/upwelling zone, with relatively lower OPE concentrations throughout the water
325 column between the estuary and the continental shelf (sites A1-1~A1-4 & A2-1~A2-4).
326 Due to the dominance of dissolved OPEs, they generally showed similar spatial
327 distribution with Σ_{12} OPEs (Figure S4). As for the particulate OPEs, their concentrations
328 gradually decreased in the water column from the estuary to the continental shelf (Figure
329 S5).



330

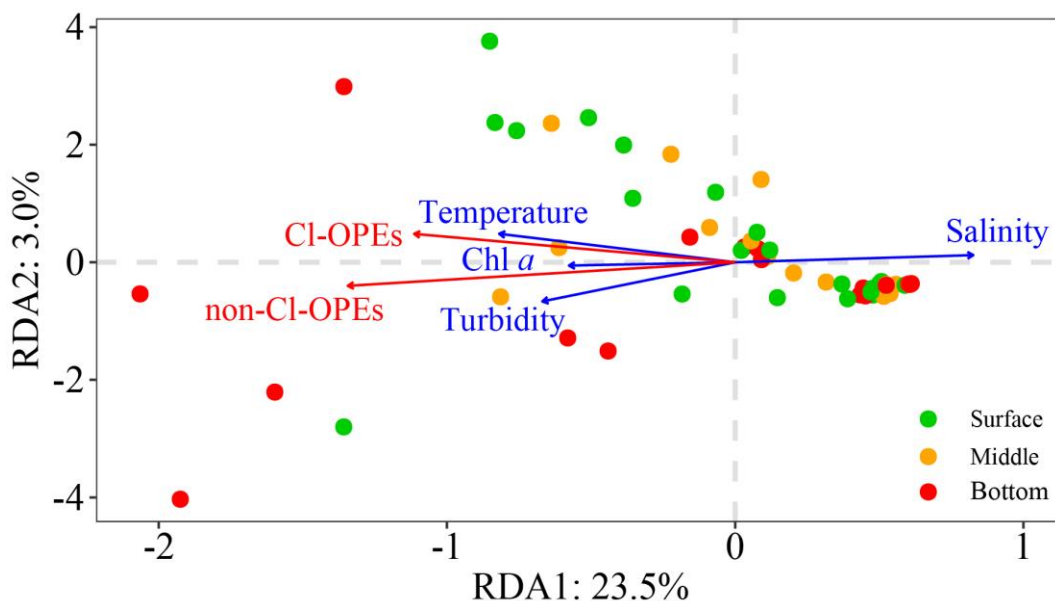
331 Figure 5. Vertical profiles of the total concentration of dissolved and particulate OPEs in water of the
 332 Changjiang River estuary. The concentration of Σ_{12} OPEs (b), Σ_3 Cl-OPEs (c) and Σ_9 non-Cl-OPEs (d)
 333 in transect B-C-A1 (a, n = 41); and the concentration of Σ_{12} OPEs (f), Σ_3 Cl-OPEs (g) and Σ_9 non-Cl-
 334 OPEs (h) in transect A2 (e, n = 20); white points represent the laboratory measurement data

335

336 3.3 Physical and biogeochemical drivers of OPE concentrations

337 For RDA, scaled explanatory variables were grouped according to likely regional
 338 drivers of contaminant accumulation: (i) sediment input to the estuary was represented by
 339 turbidity; (ii) salinity to distinguish seawater from freshwater and to indicate the riverine
 340 input; (iii) temperature and salinity indicated the summertime stratification and upwelling
 341 process; (iv) Chl *a* implied the potential effects of the biological pump. For all samples (n

342 = 61), RDA constraining variables explained a considerable amount of OPE variations in
343 our study area (27%, permutation test: $p = 0.001$; Figure 6), with the first axis of 24%
344 (permutation test: $p = 0.002$) and the second axis of only 3%. The OPE variations were
345 significantly/positively explained by environmental variables including temperature,
346 turbidity and Chl *a*, but negatively explained by salinity. Due to the complexity of the
347 topographic and hydrodynamic conditions of the Changjiang River estuary, the
348 predominant environmental variables differed greatly across the estuary,
349 frontal/upwelling zone, and continental shelf region. In the estuarine sites ($n = 22$), the
350 constraining variables only explained ~4% of the variation in OPE concentrations, and
351 the RDA model showed non-significance possibly due to the homogeneity in temperature,
352 salinity and Chl *a* at these estuarine sites. For the frontal/upwelling zone ($n = 23$), RDA
353 constraining variables explained 52% of the variance in OPE concentrations (permutation
354 test: $p = 0.03$; Figure S6a), with significant Chl *a*, turbidity and salinity contributions. Chl
355 *a* also had significant impact on the variance of OPEs in the continental shelf region, in
356 which 22% was explained by the RDA constraining variables ($n = 16$, permutation test: p
357 = 0.04; Figure S6b).



358

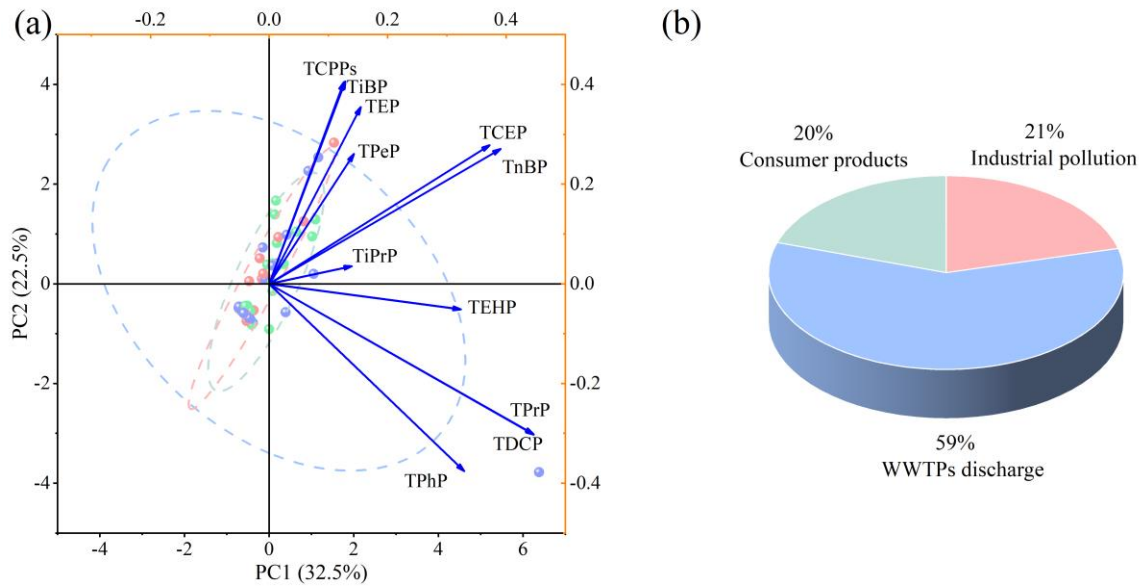
359 Figure 6. Transformation-based redundancy analysis (RDA) based on the concentrations of non-CI-
 360 OPEs and CI-OPEs (in red). Constraining variables: salinity, temperature, turbidity and Chl *a*, are
 361 shown in blue. Each point represents one individual sample, and color represents the sampling depth
 362 in each station (n = 61)

363

364 3.4 Source apportionments of OPEs

365 Three significant factors were identified from the PCA analysis, which explained
 366 33%, 22% and 12% of the total variability of the original OPEs dataset, respectively
 367 (Table S9 and Table S10). PC1 was predominantly weighted by TCEP, TDCP, TPrP,
 368 TnBP, TEHP and TPhP (Figure 7a), which could be explained as industrial pollution,
 369 because these OPEs were widely used as sealants, coating products and lubricants (Van
 370 der Veen & de Boer, 2012). PC2 was mainly associated with some more hydrophilic
 371 compounds with relatively lower log K_{OW} values, including TCPPs, TiBP and TPeP. Thus,
 372 PC2 could be related to WWTPs discharge (Kim et al., 2017; Schreder & La Guardia,
 373 2014). PC3 was predominantly composed of TEP and TiPrP, which were mainly used as

374 plasticizer additives and could originate from indoor environments (Blum et al., 2019).
 375 Therefore, PC3 could be regarded as consumer products' signature. Moreover, the
 376 following MLR results showed that the mean contributions were 59% for the WWTPs
 377 discharge, 21% for the industrial pollution and 20% for consumer products, respectively
 378 (Figure 7b).



379
 380 Figure 7. PCA results of OPEs in all water samples, and the dashed line represents the 95% confidence
 381 ellipse (a); Contributions of three potential sources obtained from MLR (b)

382

383 3.5 Riverine mass input to the ECS

384 The Changjiang River runoff was estimated as 117.8 billion cubic meters during July,
 385 2021, and the corresponding daily mass input of dissolved OPEs ($\Sigma_{12}OPEs_{dis}$) from the
 386 estuary into the adjacent ECS was calculated to be 2.1 ± 0.79 t/d. TCPPs had the highest
 387 riverine mass inflow (1.4 ± 0.65 t/d), followed by TCEP (0.42 ± 0.16 t/d) and TEP (0.17
 388 ± 0.15 t/d) respectively, probably due to the higher production and application of these
 389 compounds (Huang et al., 2022). Our results were lower than OPEs transported to the

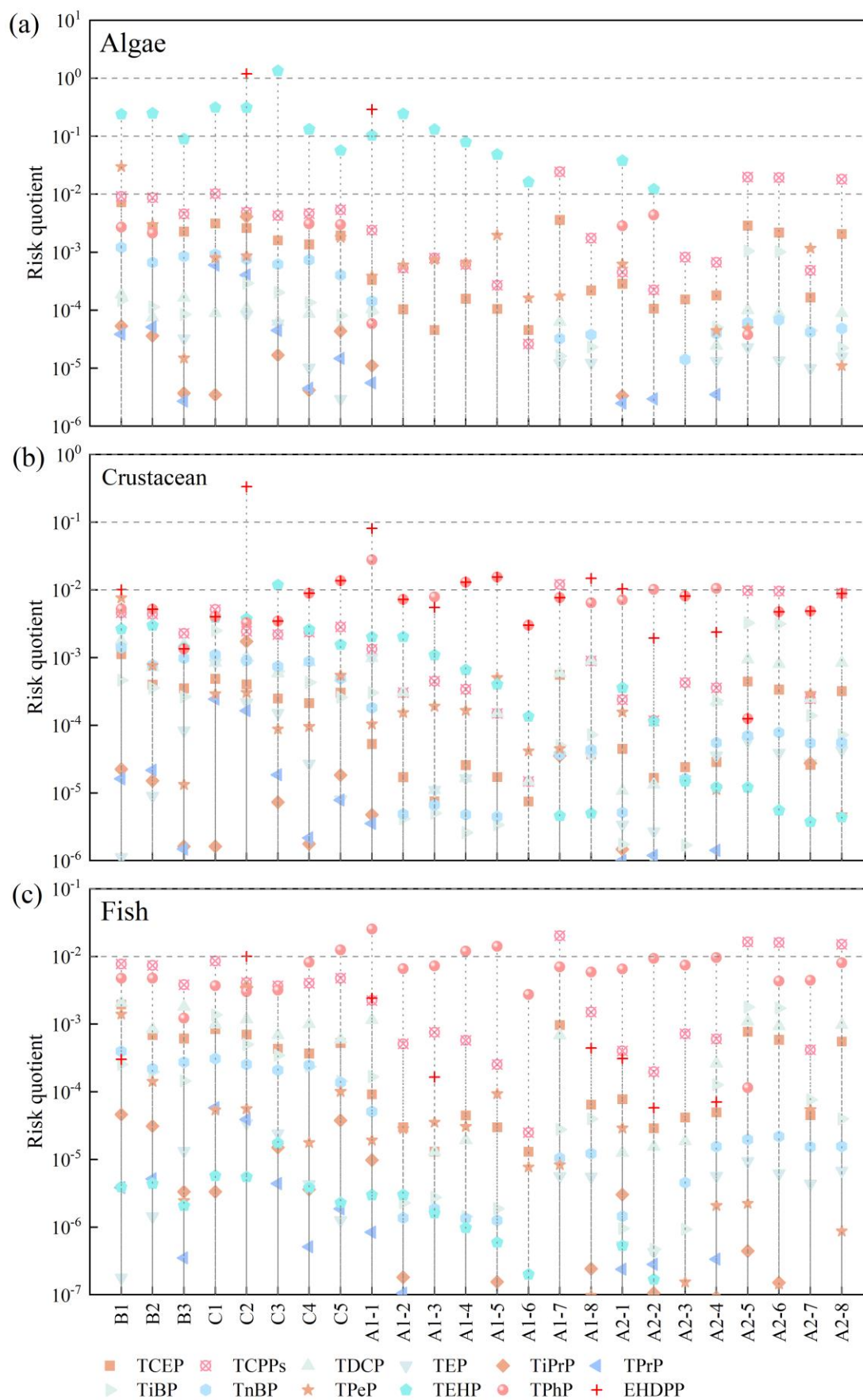
390 South China Sea via eight tributaries of the Pearl River Estuary ($\Sigma_9\text{OPEs}_{\text{dis}}$, 16 t/d),
391 probably due to several of the worlds' largest manufacturing centers located upstream of
392 Pearl River Estuary (Wang et al., 2014). Yet the daily mass input of dissolved OPEs from
393 Changjiang River observed in this study was significantly higher than the inflow of OPEs
394 through forty rivers into the Bohai Sea in northern China ($\Sigma_{11}\text{OPEs}_{\text{dis}}$, 44 ± 8.8 kg/d)
395 (Wang et al., 2015), as well as OPEs transported into the German North Sea via the
396 Rhine-Meuse delta and Elbe estuary ($\Sigma_8\text{OPEs}_{\text{dis}}$, 140 kg/d) (Bollmann et al., 2012) and to
397 the Gulf of Lion by the Rhône River ($\Sigma_8\text{OPEs}_{\text{dis}}$, 10-116 kg/d) (Schmidt et al., 2020).
398 Notably, the massive sediment inputs also played a crucial role in carrying OPEs into the
399 ECS. The mass inflow of particulate OPEs ($\Sigma_{12}\text{OPEs}_{\text{par}}$) was estimated as 72 ± 45 kg/d,
400 comparable with those estimated in the Pearl River Estuary ($\Sigma_{10}\text{OPEs}_{\text{par}}$, 65 kg/d) (Lao et
401 al., 2022). The dominant compounds for particulate inflow were TCPPs (38 ± 23 kg/d)
402 and TPhP (14 ± 15 kg/d), respectively.

403

404 **3.6 Ecological risk assessment of OPEs**

405 As the primary producers of aquatic ecosystems, algae are most sensitive to
406 anthropogenic OPEs. The dissolved OPEs posed high-moderate risk to algae at some
407 estuarine sites, with $RQs > 1$ at sites C2 & C3, and $0.1 < RQs < 1.0$ at sites B1, B2, C1,
408 C4, A1-1 to A1-3, while no significant or low risks were present at the other sites off the
409 estuary ($RQs < 0.1$) (Figure 8a). Except for the C2 station, the OPEs posed low or no
410 significant risk to crustaceans and fish (Figure 8b-8c). For individual OPE compounds,
411 TPhP, TCPPs and EHDPP posed greater ecological threat to fish and crustaceans due to
412 their elevated concentrations. In contrast, TEHP posed greater ecological risks to algae

413 than other individual OPEs, due to its relative lower PNEC value (Table S11).



415 Figure 8. Risk quotients of individual OPE on algae (a), crustaceans (b) and fish (c) in surface water
416 from the Changjiang River estuary. The values of horizontal dashed line indicate the ecological risk
417 thresholds: no significant impact ($RQ < 0.01$), low ($0.01 < RQ < 0.1$), medium ($0.1 < RQ < 1.0$) and
418 high ($RQ > 1.0$)

419

420 **4. DISCUSSION**

421 **4.1 Combined effects of fronts, upwelling and the biological pump**

422 The physical and biogeochemical characteristics of the Changjiang River estuary
423 and its adjacent coastal regions were highly variable in summer. The inputs of land runoff
424 from the Changjiang River carried large amount of sediments and nutrients into the ECS,
425 and formed the frontal area at the confluence of Changjiang diluted freshwater and
426 seawater (Gao et al., 2015). Phytoplankton are known to preferentially accumulate in this
427 region, benefitting from rich nutrients, sufficient light and suitable temperature (Ge et al.,
428 2020). Additionally, the co-existed coastal upwellings also contributed to the supply of
429 nutrients, and thus phytoplankton accumulation (Largier, 2020; Pei et al., 2009). In this
430 study, the relatively higher OPE concentrations shown in the bottom water of the
431 estuarine and frontal zones coincided exactly with the high turbidity regions. The RDA
432 results also indicated the significant influence of turbidity in the study area (Figure 6).
433 The bottom water with high turbidity could be due to either the massive inflow and
434 accumulation of terrestrial sediments (B1 & C1), or the algal growth and subsequent
435 sedimentation of biogenic particles (A1-1). The estuarine sediment is deemed a regional
436 sink of terrestrial pollutants (Barletta et al., 2019), and the typically positive correlation
437 between particulate OPEs and SPM (Pearson test, $r = 0.45$, $p = 0.03$) at estuarine sites
438 (B1-B3 & C1-C5) further demonstrated the sedimentation capturing OPEs in this region.

439 In the frontal/upwelling and continental shelf area (A1-1 to A1-8 & A2-1 to A2-8), Chl *a*
440 in seawater was significantly and positively correlated with SPM (Pearson test, $r = 0.56$,
441 $p < 0.01$), indicating the contribution of planktonic particulate matter to SPM. The
442 Σ_{12} OPEs in seawater was significantly and positively correlated with Chl *a* (Pearson test,
443 $r = 0.32$, $p < 0.04$), but not with SPM. The RDA analysis also suggested the importance
444 of Chl *a*, an indicator of the biological pump, in both frontal/upwelling and continental
445 shelf regions. Therefore, some comparable higher OPE concentrations in the intermediate
446 and bottom layers with high Chl *a* (A1-1, A1-4 and A2-6) could have resulted from the
447 biological pump. Specifically, the OPEs attached to particulate organic matter produced
448 by actively growing phytoplankton in the surface layer, and were gradually released
449 during the settling process.

450 The enrichment of OPEs in the surface layer of the continental shelf (A1-7, A2-5,
451 A2-6 and A2-8) region could be due to non-point sources - their continuous inputs from
452 atmospheric deposition and riverine runoff/WWTPs discharge, as well as some point
453 sources, such as microplastic releases (Sørensen et al., 2021). The strong seasonal
454 thermocline and halocline/enhanced stratification that formed in summer further inhibited
455 the vertical mixing of the contaminants, which resulted in relatively low concentrations
456 of target contaminants in the intermediate and bottom layers of the continental shelf
457 region. The vertical profile sampling in the continental shelf area was conducted at every
458 other station, so no vertical profile observation was conducted at station A2-5, the peak
459 position of Chl *a* (8.7 $\mu\text{g/L}$) of this transect. Notably, at the Chl *a* sub-peak position (A2-6,
460 1.1 $\mu\text{g/L}$) of this transect, the coupling between deposition of OPEs with the biological
461 pump was obvious. The influence of the biological pump on the vertical transport of

462 hydrophobic organic contaminants, including polychlorinated biphenyls (PCBs), high
463 molecular weight polycyclic aromatic hydrocarbons (PAHs) and legacy organochlorine
464 pesticides (OCPs), has already been demonstrated in aquatic ecosystem (Galbán-Malagón
465 et al., 2013; González-Gaya et al., 2019; Nizzetto et al., 2012).

466

467 **4.2 Comparison analysis and other potential drivers**

468 Since most previous studies concentrated on dissolved OPEs, which also dominated
469 in this study, a specialized comparison was conducted for dissolved OPEs. The dissolved
470 OPE concentrations of this study (340 ± 380 ng/L) were comparable to the mean OPE
471 concentrations in worldwide coastal waters, such as the German Bight (400 ng/L) (Wang
472 et al., 2020) and the Amazon River mouth (460 ng/L) (Schmidt et al., 2019), but higher
473 than those observed in the open West Pacific Ocean (25 ng/L) (Xiao et al., 2021) and the
474 remote North Atlantic-Arctic Ocean (2.9 ng/L) (Li et al., 2017) (Table S12). However,
475 compared to previous studies on dissolved OPEs in the surface water of coastal China
476 Seas, our results were overall comparable but slightly lower than the mean OPE
477 concentrations detected in the Lianyungang (570 ng/L) (Hu et al., 2014), Pearl River
478 Estuary (630 ng/L), Yellow River Estuary (870 ng/L) (Lai et al., 2019) and Laizhou Bay
479 (1200 ng/L) (Lian et al., 2021).

480 The reduced level of OPEs detected in this study could be attributed to multiple
481 factors. First of all, the sampling period of this study, from July 12th to July 17th, is the
482 typical flood season. The summer runoff flux of the Changjiang River contributed ~70%
483 of its annual runoff (<http://www.cjw.gov.cn/zwzc/bmgb/>). As a result, the large amounts
484 of freshwater inputs diluted the pollutants in coastal regions. Secondly, the difference in

485 solubility of OPEs in freshwater and seawater, termed the ‘salting-out’ effect, can result
486 in enhanced volatilization (or settling) of dissolved OPE in the frontal zone. The ‘salting
487 out’/volatilization of dissolved Cl-OPEs in the frontal zone of freshwater and seawater
488 has already been observed at the mouth of the Nelson and Churchill Rivers of the
489 Canadian Arctic (Sühring et al., 2016). Additionally, the OPEs might be diluted by TWC
490 waters, which traversed a long distance from the Taiwan Strait and upwelled to the
491 surface/subsurface in the Changjiang River mouth (Wei et al., 2021). Although there is
492 currently no direct observation of summertime OPEs in TWC bottom waters, the strong
493 stratification in subtropical area during summer is very likely to cause low OPE
494 concentrations in bottom water as discussed above (Sanganyado et al., 2021). Moreover,
495 some OPEs in the study area might, at least partially, have already been microbially
496 hydrolyzed to inorganic phosphate ($\text{PO}_4\text{-P}$). The relatively low $\text{PO}_4\text{-P}$ concentration and
497 high N/P ratio in the study area indicated that $\text{PO}_4\text{-P}$ was the potentially limiting nutrient
498 in the Changjiang River estuary, especially during the sampling period of summer after
499 the conventional spring bloom (Figure 2 & 3). The alkaline phosphatase, mainly
500 produced by microorganism, can be induced under phosphorus-limited conditions. The
501 dissolved OPEs, components of dissolved organic phosphorus, can be microbially
502 hydrolyzed by alkaline phosphatase to inorganic $\text{PO}_4\text{-P}$ (Xie et al., 2021), further
503 promoting the primary productivity in aquatic environment. Although OPEs inhibit the
504 activity of acetylcholine esterase (AChE), which play an important role in biological
505 nervous system, by covalently binding to its active site, OPEs do not adversely affect
506 bacteria, because bacteria do not possess AChE, and some microorganisms can even use
507 OPEs as an energy source (Singh & Walker, 2006). Both the laboratory and in-situ

508 incubation experiments demonstrated increasing alkaline phosphatase activity (APA)
509 under phosphorus stress (Vila-Costa et al., 2019; Xie et al., 2021). Overall, the regions
510 with reduced OPE levels could be attributed to the dilution of large amount of freshwater
511 in summer, potential microbial degradation induced by phosphorus limitation, heaving of
512 deepwater containing depleted OPEs, as well as the ‘salting-out’ effects, though further
513 large-scale simultaneous air-water observations are still warranted.

514 As for the ecological risk, it appeared to be reduced due to these relatively lower
515 OPE concentrations. However, the frontal and upwelling regions are regularly
516 characterized by rich nutrients and high biological productivity, and good fishing grounds
517 are commonly found in their vicinity (Largier, 2020). Therefore, the long-term
518 ecotoxicity caused by the mixtures of OPEs cannot be ignored, considering the
519 continuous high production, application and release of OPEs to the complex coastal
520 environment (Vasseghian et al., 2022), as well as the bioaccumulation and
521 biomagnification effects of some OPEs (such as EHDPP and TPhP) (Ding et al., 2020;
522 Wang et al., 2019).

523

524 **5. CONCLUSION**

525 Dissolved and particulate OPEs were widely detected in the Changjiang River
526 estuary. Concentrations were dominated by dissolved OPEs, and the water-particle
527 partitioning of OPEs was strongly influenced by hydrophobic interactions. In contrast to
528 non-Cl-OPEs, Cl-OPEs generally exhibited relatively higher detection frequencies and
529 concentrations. Source apportionment suggested that the dominant OPE sources were
530 WWTPs discharge, although there was also evidence of industrial emissions and release

531 from consumer products. In this study, we found that the OPEs generally posed a low
532 ecological risk to aquatic life, but the long-term risks may not be insignificant as the
533 exposure continues due to their constant high production and application.

534 Due to the complex hydrological and biogeochemical processes in the Changjiang
535 River estuary, the vertical and horizontal occurrence and transport of OPEs displayed
536 great spatial variability. OPE concentrations in the estuary were high, especially for the
537 bottom waters, due to the massive terrestrial/sediment inputs; while the ‘surface
538 enrichment and depth depletion’ of OPEs in the continental shelf was influenced by
539 seasonal stratification. Overall, the water column in the frontal/upwelling zone had low
540 OPE concentrations. However, the fronts/upwelling activity could induce phytoplankton
541 blooms, and elevated OPEs were found just below the surface water where phytoplankton
542 aggregated, indicating the combined impacts of frontal/upwelling and the biological
543 pump. Considering the broad range in the physicochemical properties of OPEs, they can
544 serve as tracers of competing biogeochemical and physical oceanographic processes.
545 Some (mobile) OPEs basically trace water mass movement, while others are transported
546 by sediments or move with plankton.

547 The Changjiang River estuary proved to be an ideal region to study the influence of
548 coupled hydrological-biogeochemical processes on the OPE transport, because it is well
549 characterized for its oceanographic processes, but is also strongly impacted by OPE
550 emissions. The physical and biogeochemical processes discussed in this study, including
551 riverine inputs, fronts and coastal upwellings, as well as the biological pump and
552 biodegradation, are typical for global estuaries. Therefore, our methods, results and
553 conclusions here could be generalized to assess the complicated environmental behavior

554 and fate of OPEs in other estuarine and coastal regions around the world.

555

556 **Acknowledgments**

557 This research is supported by National Natural Science Foundation of China (NSFC,
558 Grant No. 41976211). Data and samples were collected onboard of R/V *Zheyuke 2*
559 implementing the open research cruise NORC2021-03 supported by NSFC Shiptime
560 Sharing Project (Project No. 42049903).

561

562 **Open Research**

563 **Data Availability Statement**

564 All data, including experiment details, instrument conditions, sampling information,
565 physicochemical properties of OPEs, QA/QC and detail OPE concentrations have been
566 deposited in ZENODO (<https://doi.org/10.5281/zenodo.8418167>). The above dataset is
567 also available in the supporting information.

568

569 **REFERENCE**

570 Bai, X., & Hu, D. (2004). A numerical study on seasonal variations of the Taiwan Warm

571 Current. *Chinese Journal of Oceanology and Limnology*, 22(3), 278-285.

572 doi:<https://doi.org/10.1007/BF02842560>

573 Barletta, M., Lima, A. R. A., & Costa, M. F. (2019). Distribution, sources and

574 consequences of nutrients, persistent organic pollutants, metals and microplastics in

575 South American estuaries. *Science of the Total Environment*, 651, 1199-1218.

576 doi:<https://doi.org/10.1016/j.scitotenv.2018.09.276>

577 Blum, A., Behl, M., Birnbaum, L. S., Diamond, M. L., Phillips, A., Singla, V., et al.

- 578 (2019). Organophosphate ester flame retardants: Are they a regrettable substitution
579 for polybrominated diphenyl ethers? *Environmental Science & Technology Letters*,
580 6(11), 638-649. doi:<https://doi.org/10.1021/acs.estlett.9b00582>
- 581 Bollmann, U. E., Möller, A., Xie, Z., Ebinghaus, R., & Einax, J. W. (2012). Occurrence
582 and fate of organophosphorus flame retardants and plasticizers in coastal and marine
583 surface waters. *Water Research*, 46(2), 531-538.
584 doi:<https://doi.org/10.1016/j.watres.2011.11.028>
- 585 Cao, D., Guo, J., Wang, Y., Li, Z., Liang, K., Corcoran, M. B., et al. (2017).
586 Organophosphate esters in sediment of the Great Lakes. *Environmental Science &*
587 *Technology*, 51(3), 1441-1449. doi:<https://doi.org/10.1021/acs.est.6b05484>
- 588 Castro-Jiménez, J., Berrojalbiz, N., Pizarro, M., & Dachs, J. (2014). Organophosphate
589 ester (OPE) flame retardants and plasticizers in the open Mediterranean and Black
590 Seas atmosphere. *Environmental Science & Technology*, 48(6), 3203-3209.
591 doi:<https://doi.org/10.1021/es405337g>
- 592 Chen, L., Xiao, Y., Li, Y., & Shen, Z. (2018). Construction of the hydrological condition-
593 persistent organic pollutants relationship in the Yangtze River Estuary. *Journal of*
594 *Hazardous Materials*, 360, 544-551.
595 doi:<https://doi.org/10.1016/j.jhazmat.2018.08.045>
- 596 Chen, M., Gan, Z., Qu, B., Chen, S., Dai, Y., & Bao, X. (2019). Temporal and seasonal
597 variation and ecological risk evaluation of flame retardants in seawater and
598 sediments from Bohai Bay near Tianjin, China during 2014 to 2017. *Marine*
599 *Pollution Bulletin*, 146, 874-883.
600 doi:<https://doi.org/10.1016/j.marpolbul.2019.07.049>

- 601 Chen, S.-L., Zhang, G.-A., Yang, S.-L., & Shi, J. Z. (2006). Temporal variations of fine
602 suspended sediment concentration in the Changjiang River estuary and adjacent
603 coastal waters, China. *Journal of Hydrology*, 331(1), 137-145.
604 doi:<https://doi.org/10.1016/j.jhydrol.2006.05.013>
- 605 Ding, Y., Han, M., Wu, Z., Zhang, R., Li, A., Yu, K., et al. (2020). Bioaccumulation and
606 trophic transfer of organophosphate esters in tropical marine food web, South China
607 Sea. *Environment International*, 143, 105919.
608 doi:<https://doi.org/10.1016/j.envint.2020.105919>
- 609 Dong, H., Zhou, M., Hu, Z., Zhang, Z., Zhong, Y., Basedow, S. L., et al. (2021).
610 Transport barriers and the retention of *Calanus finmarchicus* on the Lofoten shelf in
611 early spring. *Journal of Geophysical Research: Oceans*, 126(8), e2021JC017408.
612 doi:<https://doi.org/10.1029/2021JC017408>
- 613 Fang, L., Liu, A., Zheng, M., Wang, L., Hua, Y., Pan, X., et al. (2022). Occurrence and
614 distribution of organophosphate flame retardants in seawater and sediment from
615 coastal areas of the East China and Yellow Seas. *Environmental Pollution*, 302,
616 119017. doi:<https://doi.org/10.1016/j.envpol.2022.119017>
- 617 Galbán-Malagón, C. J., Del Vento, S., Berrojalbiz, N., Ojeda, M. J., & Dachs, J. (2013).
618 Polychlorinated biphenyls, hexachlorocyclohexanes and hexachlorobenzene in
619 seawater and phytoplankton from the Southern Ocean (Weddell, South Scotia, and
620 Bellingshausen Seas). *Environmental Science & Technology*, 47(11), 5578-5587.
621 doi:<https://doi.org/10.1021/es400030q>
- 622 Gao, L., Li, D., Ishizaka, J., Zhang, Y., Zong, H., & Guo, L. (2015). Nutrient dynamics
623 across the river-sea interface in the Changjiang (Yangtze River) estuary East China

- 624 Sea region. *Limnology and Oceanography*, 60(6), 2207-2221. doi:
 625 <https://doi.org/10.1002/lno.10196>
- 626 Ge, J., Shi, S., Liu, J., Xu, Y., Chen, C., Bellerby, R., et al. (2020). Interannual
 627 variabilities of nutrients and phytoplankton off the Changjiang Estuary in response
 628 to Changing River Inputs. *Journal of Geophysical Research: Oceans*, 125(3),
 629 e2019JC015595. doi:<https://doi.org/10.1029/2019JC015595>
- 630 González-Gaya, B., Martínez-Varela, A., Vila-Costa, M., Casal, P., Cerro-Gálvez, E.,
 631 Berrojalbiz, N., et al. (2019). Biodegradation as an important sink of aromatic
 632 hydrocarbons in the oceans. *Nature Geoscience*, 12(2), 119-125.
 633 doi:<https://doi.org/10.1038/s41561-018-0285-3>
- 634 Gravel, S., Lavoué, J., Bakhiyi, B., Diamond, M. L., Jantunen, L. M., Lavoie, J., et al.
 635 (2019). Halogenated flame retardants and organophosphate esters in the air of
 636 electronic waste recycling facilities: Evidence of high concentrations and multiple
 637 exposures. *Environment International*, 128, 244-253.
 638 doi:<https://doi.org/10.1016/j.envint.2019.04.027>
- 639 He, T., Qing, X., Chen, X., Wang, W., Junaid, M., Gao, B., et al. (2022). The coupling
 640 between biological pump export and air-water exchange of organophosphate esters
 641 in a subtropical water environment. *Science of the Total Environment*, 853, 158623.
 642 doi:<https://doi.org/10.1016/j.scitotenv.2022.158623>
- 643 Hu, J., & Wang, X. H. (2016). Progress on upwelling studies in the China seas. *Reviews*
 644 *of Geophysics*, 54(3), 653-673. doi:<https://doi.org/10.1002/2015rg000505>
- 645 Hu, M., Li, J., Zhang, B., Cui, Q., Wei, S., & Yu, H. (2014). Regional distribution of
 646 halogenated organophosphate flame retardants in seawater samples from three

- 647 coastal cities in China. *Marine Pollution Bulletin*, 86(1-2), 569-574.
648 doi:<https://doi.org/10.1016/j.marpolbul.2014.06.009>
- 649 Huang, J., Ye, L., Fang, M., & Su, G. (2022). Industrial production of organophosphate
650 flame retardants (OPFRs): Big knowledge gaps need to be filled? *Bulletin of*
651 *Environmental Contamination and Toxicology*, 108.
652 doi:<https://doi.org/10.1007/s00128-021-03454-7>
- 653 Kim, U. J., Oh, J. K., & Kannan, K. (2017). Occurrence, removal, and environmental
654 emission of organophosphate flame retardants/plasticizers in a wastewater treatment
655 plant in New York State. *Environmental Science & Technology*, 51(14), 7872-7880.
656 doi:<https://doi.org/10.1021/acs.est.7b02035>
- 657 Lai, N. L. S., Kwok, K. Y., Wang, X. H., Yamashita, N., Liu, G., Leung, K. M. Y., et al.
658 (2019). Assessment of organophosphorus flame retardants and plasticizers in aquatic
659 environments of China (Pearl River Delta, South China Sea, Yellow River Estuary)
660 and Japan (Tokyo Bay). *Journal of Hazardous Materials*, 371, 288-294.
661 doi:<https://doi.org/10.1016/j.jhazmat.2019.03.029>
- 662 Lao, J.-Y., Wu, R., Cui, Y., Zhou, S., Ruan, Y., Leung, K. M. Y., et al. (2022). Significant
663 input of organophosphate esters through particle-mediated transport into the Pearl
664 River Estuary, China. *Journal of Hazardous Materials*, 438, 129486.
665 doi:<https://doi.org/10.1016/j.jhazmat.2022.129486>
- 666 Largier, J. L. (2020). Upwelling bays: How coastal upwelling controls circulation, habitat,
667 and productivity in bays. *Annual Review of Marine Science*, 12(1), 415-447.
668 doi:<https://doi.org/10.1146/annurev-marine-010419-011020>
- 669 Li, J., Tang, J., Mi, W., Tian, C., Emeis, K.-C., Ebinghaus, R., et al. (2018). Spatial

- 670 distribution and seasonal variation of organophosphate esters in air above the Bohai
 671 and Yellow Seas, China. *Environmental Science & Technology*, 52(1), 89-97.
 672 doi:<https://doi.org/10.1021/acs.est.7b03807>
- 673 Li, J., Xie, Z., Mi, W., Lai, S., Tian, C., Emeis, K. C., et al. (2017). Organophosphate
 674 esters in air, snow, and seawater in the North Atlantic and the Arctic. *Environmental*
 675 *Science & Technology*, 51(12), 6887-6896.
 676 doi:<https://doi.org/10.1021/acs.est.7b01289>
- 677 Li, S., Zhang, Z., Zhou, M., Wang, C., Wu, H., & Zhong, Y. (2022). The role of fronts in
 678 horizontal transports of the Changjiang River plume in summer and the Implications
 679 for phytoplankton blooms. *Journal of Geophysical Research-Oceans*, 127(8).
 680 doi:<https://doi.org/10.1029/2022jc018541>
- 681 Lian, M., Lin, C., Wu, T., Xin, M., Gu, X., Lu, S., et al. (2021). Occurrence,
 682 spatiotemporal distribution, and ecological risks of organophosphate esters in the
 683 water of the Yellow River to the Laizhou Bay, Bohai Sea. *The Science of the total*
 684 *environment*, 787, 147528-147528.
 685 doi:<https://doi.org/10.1016/j.scitotenv.2021.147528>
- 686 Liu, J. P., Xu, K. H., Li, A. C., Milliman, J. D., Velozzi, D. M., Xiao, S. B., et al. (2007).
 687 Flux and fate of Yangtze river sediment delivered to the East China Sea.
 688 *Geomorphology*, 85(3-4), 208-224.
 689 doi:<https://doi.org/10.1016/j.geomorph.2006.03.023>
- 690 Liu, Y., Deng, B., Du, J., Zhang, G., & Hou, L. (2019). Nutrient burial and environmental
 691 changes in the Yangtze Delta in response to recent river basin human activities.
 692 *Environmental Pollution*, 249, 225-235.

- 693 doi:<https://doi.org/10.1016/j.envpol.2019.03.030>
- 694 Ma, Y., Luo, Y., Zhu, J., Zhang, J., Gao, G., Mi, W., et al. (2022). Seasonal variation and
695 deposition of atmospheric organophosphate esters in the coastal region of Shanghai,
696 China. *Environmental Pollution*, 300.
697 doi:<https://doi.org/10.1016/j.envpol.2022.118930>
- 698 Nizzetto, L., Gioia, R., Li, J., Borgå, K., Pomati, F., Bettinetti, R., et al. (2012).
699 Biological pump control of the fate and distribution of hydrophobic organic
700 pollutants in water and plankton. *Environmental Science & Technology*, 46(6), 3204-
701 3211. doi:<https://doi.org/10.1021/es204176q>
- 702 Olivero-Verbel, R., Johnson-Restrepo, B., & Eljarrat, E. (2022). Human exposure
703 assessment of organophosphate esters (OPEs) through dust ingestion and dermal
704 absorption in Colombian cities. *Journal of Environmental Exposure Assessment*,
705 1(2), 8. doi:<https://doi.org/10.20517/jeea.2021.08>
- 706 Pantelaki, I., & Voutsas, D. (2021). Organophosphate esters in inland and coastal waters in
707 northern Greece. *Science of the Total Environment*, 800, 149544.
708 doi:<https://doi.org/10.1016/j.scitotenv.2021.149544>
- 709 Pei, S., Shen, Z., & Laws, E. A. (2009). Nutrient dynamics in the upwelling area of
710 Changjiang (Yangtze River) Estuary. *Journal of Coastal Research*, 25(3), 569-580.
711 doi:<https://doi.org/10.2112/07-0948.1>
- 712 Quintana, J. B., Rodil, R., Reemtsma, T., García-López, M., & Rodríguez, I. (2008).
713 Organophosphorus flame retardants and plasticizers in water and air II. Analytical
714 methodology. *TrAC Trends in Analytical Chemistry*, 27(10), 904-915.
715 doi:<https://doi.org/10.1016/j.trac.2008.08.004>

- 716 Rodgers, T. F. M., Truong, J. W., Jantunen, L. M., Helm, P. A., & Diamond, M. L. (2018).
717 Organophosphate ester transport, fate, and emissions in Toronto, Canada, estimated
718 using an updated multimedia urban model. *Environmental Science & Technology*,
719 52(21), 12465-12474. doi:<https://doi.org/10.1021/acs.est.8b02576>
- 720 Sanganyado, E., Chingono, K. E., Gwenzi, W., Chaukura, N., & Liu, W. H. (2021).
721 Organic pollutants in deep sea: Occurrence, fate, and ecological implications. *Water*
722 *Research*, 205. doi:<https://doi.org/10.1016/j.watres.2021.117658>
- 723 Schmidt, N., Castro-Jiménez, J., Fauvelle, V., Ourgaud, M., & Sempéré, R. (2020).
724 Occurrence of organic plastic additives in surface waters of the Rhône River
725 (France). *Environmental Pollution*, 257, 113637.
726 doi:<https://doi.org/10.1016/j.envpol.2019.113637>
- 727 Schmidt, N., Fauvelle, V., Ody, A., Castro-Jiménez, J., Jouanno, J., Changeux, T., et al.
728 (2019). The Amazon River: A major source of organic plastic additives to the
729 tropical North Atlantic? *Environmental Science & Technology*, 53(13), 7513-7521.
730 doi:<https://doi.org/10.1021/acs.est.9b01585>
- 731 Schreder, E. D., & La Guardia, M. J. (2014). Flame retardant transfers from U.S.
732 households (dust and laundry wastewater) to the aquatic environment.
733 *Environmental Science & Technology*, 48(19), 11575-11583.
734 doi:<https://doi.org/10.1021/es502227h>
- 735 Shi, Y., Zhang, Y., Du, Y., Kong, D., Wu, Q., Hong, Y., et al. (2020). Occurrence,
736 composition and biological risk of organophosphate esters (OPEs) in water of the
737 Pearl River Estuary, South China. *Environmental Science and Pollution Research*,
738 27(13), 14852-14862. doi:<https://doi.org/10.1007/s11356-020-08001-1>

- 739 Shimabuku, I., Chen, D., Wu, Y., Miller, E., Sun, J., & Sutton, R. (2022). Occurrence and
 740 risk assessment of organophosphate esters and bisphenols in San Francisco Bay,
 741 California, USA. *Science of the Total Environment*, 813, 152287.
 742 doi:<https://doi.org/10.1016/j.scitotenv.2021.152287>
- 743 Simpson, J. H., Edelman, D. J., Edwards, A., Morris, N. C. G., & Tett, P. B. (1979). The
 744 Islay front: Physical structure and phytoplankton distribution. *Estuarine and Coastal
 745 Marine Science*, 9(6), 713-711. doi:[https://doi.org/10.1016/S0302-
 746 3524\(79\)80005-5](https://doi.org/10.1016/S0302-3524(79)80005-5)
- 747 Singh, B. K., & Walker, A. (2006). Microbial degradation of organophosphorus
 748 compounds. *Fems Microbiology Reviews*, 30(3), 428-471.
 749 doi:<http://doi.org/10.1111/j.1574-6976.2006.00018.x>
- 750 Sørensen, L., Groven, A. S., Hovsbakken, I. A., Del Puerto, O., Krause, D. F., Sarno, A.,
 751 et al. (2021). UV degradation of natural and synthetic microfibers causes
 752 fragmentation and release of polymer degradation products and chemical additives.
 753 *Science of the Total Environment*, 755, 143170.
 754 doi:<https://doi.org/10.1016/j.scitotenv.2020.143170>
- 755 Sühling, R., Diamond, M. L., Scheringer, M., Wong, F., Pućko, M., Stern, G., et al.
 756 (2016). Organophosphate esters in Canadian Arctic air: Occurrence, levels and
 757 trends. *Environmental Science & Technology*, 50(14), 7409-7415.
 758 doi:<https://doi.org/10.1021/acs.est.6b00365>
- 759 Van der Veen, I., & de Boer, J. (2012). Phosphorus flame retardants: Properties,
 760 production, environmental occurrence, toxicity and analysis. *Chemosphere*, 88(10),
 761 1119-1153. doi:<https://doi.org/10.1016/j.chemosphere.2012.03.067>

- 762 Vasseghian, Y., Alimohamadi, M., Khataee, A., & Dragoi, E. N. (2022). A global
 763 systematic review on the concentration of organophosphate esters in water resources:
 764 Meta-analysis, and probabilistic risk assessment. *Science of the Total Environment*,
 765 807, 150876. doi:<https://doi.org/10.1016/j.scitotenv.2021.150876>
- 766 Verbruggen, E. M. J., Rila, J. P., Traas, T. P., Posthuma-Doodeman, C. J. A. M., &
 767 Posthumus, R. (2005), Environmental risk limits for several phosphate esters, with
 768 possible application as flame retardant (*Rep. 601501024*). Bilthoven: Netherlands
 769 National Institute for Public Health and the Environment.
- 770 Vila-Costa, M., Sebastian, M., Pizarro, M., Cerro-Galvez, E., Lundin, D., Gasol, J. M., et
 771 al. (2019). Microbial consumption of organophosphate esters in seawater under
 772 phosphorus limited conditions. *Scientific Reports*, 9.
 773 doi:<https://doi.org/10.1038/s41598-018-36635-2>
- 774 Wang, R., Tang, J., Xie, Z., Mi, W., Chen, Y., Wolschke, H., et al. (2015). Occurrence and
 775 spatial distribution of organophosphate ester flame retardants and plasticizers in 40
 776 rivers draining into the Bohai Sea, north China. *Environmental Pollution*, 198, 172-
 777 178. doi:<https://doi.org/10.1016/j.envpol.2014.12.037>
- 778 Wang, X., He, Y., Lin, L., Zeng, F., & Luan, T. (2014). Application of fully automatic
 779 hollow fiber liquid phase microextraction to assess the distribution of
 780 organophosphate esters in the Pearl River Estuaries. *Science of the Total
 781 Environment*, 470-471, 263-269. doi:<https://doi.org/10.1016/j.scitotenv.2013.09.069>
- 782 Wang, X., Zhong, W., Xiao, B., Liu, Q., Yang, L., Covaci, A., et al. (2019).
 783 Bioavailability and biomagnification of organophosphate esters in the food web of
 784 Taihu Lake, China: Impacts of chemical properties and metabolism. *Environment*

- 785 *International*, 125, 25-32. doi:<https://doi.org/10.1016/j.envint.2019.01.018>
- 786 Wang, X., Zhu, L., Zhong, W., & Yang, L. (2018). Partition and source identification of
787 organophosphate esters in the water and sediment of Taihu Lake, China. *Journal of*
788 *Hazardous Materials*, 360, 43-50. doi:<https://doi.org/10.1016/j.jhazmat.2018.07.082>
- 789 Wang, X., Zhu, Q., Yan, X., Wang, Y., Liao, C., & Jiang, G. (2020). A review of
790 organophosphate flame retardants and plasticizers in the environment: Analysis,
791 occurrence and risk assessment. *Science of the Total Environment*, 731, 139071.
792 doi:<https://doi.org/10.1016/j.scitotenv.2020.139071>
- 793 Wei, Q., Yao, P., Xu, B., Zhao, B., Ran, X., Zhao, Y., et al. (2021). Coastal upwelling
794 combined with the river plume regulates hypoxia in the Changjiang Estuary and
795 adjacent inner East China Sea shelf. *Journal of Geophysical Research-Oceans*,
796 126(11). doi:<https://doi.org/10.1029/2021jc017740>
- 797 Wolschke, H., Sühring, R., Massei, R., Tang, J., & Ebinghaus, R. (2018). Regional
798 variations of organophosphorus flame retardants-Fingerprint of large river basin
799 estuaries/deltas in Europe compared with China. *Environmental Pollution*, 236, 391-
800 395. doi:<https://doi.org/10.1016/j.envpol.2018.01.061>
- 801 Wu, T., Mao, L., Liu, X., Wang, B., Lin, C., Xin, M., et al. (2021). Seasonal occurrence,
802 allocation and ecological risk of organophosphate esters in a typical urbanized semi-
803 closed bay. *Environmental Pollution*, 290.
804 doi:<https://doi.org/10.1016/j.envpol.2021.118074>
- 805 Xiao, K., Lu, Z., Yang, C., Zhao, S., Zheng, H., Gao, Y., et al. (2021). Occurrence,
806 distribution and risk assessment of organophosphate ester flame retardants and
807 plasticizers in surface seawater of the West Pacific. *Marine Pollution Bulletin*, 170.

- 808 doi:<https://doi.org/10.1016/j.marpolbul.2021.112691>
- 809 Xie, E., Su, Y., Deng, S., Kontopyrgou, M., & Zhang, D. (2021). Significant influence of
810 phosphorus resources on the growth and alkaline phosphatase activities of
811 *Microcystis aeruginosa*. *Environmental Pollution*, 268, 115807.
812 doi:<https://doi.org/10.1016/j.envpol.2020.115807>
- 813 Xu, C., Chen, L., You, L., Xu, Z., Ren, L. F., Gin, K. Y. H., et al. (2018). Occurrence,
814 impact variables and potential risk of PPCPs and pesticides in a drinking water
815 reservoir and related drinking water treatment plants in the Yangtze Estuary.
816 *Environmental Science-Processes & Impacts*, 20(7), 1030-1045.
817 doi:<https://doi.org/10.1039/c8em00029h>
- 818 Zeng, X., Liu, Z., He, L., Cao, S., Song, H., Yu, Z., et al. (2015). The occurrence and
819 removal of organophosphate ester flame retardants/plasticizers in a municipal
820 wastewater treatment plant in the Pearl River Delta, China. *Journal of*
821 *Environmental Science and Health, Part A*, 50(12), 1291-1297.
822 doi:<https://doi.org/10.1080/10934529.2015.1055158>
- 823 Zhang, L., Wang, Y., Tan, F., Yang, Y., Wu, X., Wang, W., et al. (2020). Tidal variability
824 of polycyclic aromatic hydrocarbons and organophosphate esters in the coastal
825 seawater of Dalian, China. *Science of the Total Environment*, 708.
826 doi:<https://doi.org/10.1016/j.scitotenv.2019.134441>
- 827 Zheng, H., Cai, M., Yang, C., Gao, Y., Chen, Z., & Liu, Y. (2022). Terrigenous export and
828 ocean currents' diffusion of organophosphorus flame retardants along China's
829 adjacent seas. *Environmental Pollution*, 299, 118873.
830 doi:<https://doi.org/10.1016/j.envpol.2022.118873>

831

832 **References From the Supporting Information**

833 Alvarez, D. A., Maruya, K. A., Dodder, N. G., Lao, W., Furlong, E. T., & Smalling, K. L.

834 (2014). Occurrence of contaminants of emerging concern along the California coast

835 (2009–2010) using passive sampling devices. *Marine Pollution Bulletin*, *81*(2), 347-836 354. doi:<https://doi.org/10.1016/j.marpolbul.2013.04.022>

837 Bollmann, U. E., Möller, A., Xie, Z., Ebinghaus, R., & Einax, J. W. (2012). Occurrence

838 and fate of organophosphorus flame retardants and plasticizers in coastal and marine

839 surface waters. *Water Research*, *46*(2), 531-538.840 doi:<https://doi.org/10.1016/j.watres.2011.11.028>

841 Chen, M., Gan, Z., Qu, B., Chen, S., Dai, Y., & Bao, X. (2019). Temporal and seasonal

842 variation and ecological risk evaluation of flame retardants in seawater and

843 sediments from Bohai Bay near Tianjin, China during 2014 to 2017. *Marine*844 *Pollution Bulletin*, *146*, 874-883.845 doi:<https://doi.org/10.1016/j.marpolbul.2019.07.049>

846 Cristale, J., García Vázquez, A., Barata, C., & Lacorte, S. (2013). Priority and emerging

847 flame retardants in rivers: Occurrence in water and sediment, *Daphnia magna*848 toxicity and risk assessment. *Environment International*, *59*, 232-243.849 doi:<https://doi.org/10.1016/j.envint.2013.06.011>

850 Hu, M., Li, J., Zhang, B., Cui, Q., Wei, S., & Yu, H. (2014). Regional distribution of

851 halogenated organophosphate flame retardants in seawater samples from three

852 coastal cities in China. *Marine Pollution Bulletin*, *86*(1-2), 569-574.853 doi:<https://doi.org/10.1016/j.marpolbul.2014.06.009>

- 854 Lai, N. L. S., Kwok, K. Y., Wang, X. H., Yamashita, N., Liu, G., Leung, K. M. Y., et al.
 855 (2019). Assessment of organophosphorus flame retardants and plasticizers in aquatic
 856 environments of China (Pearl River Delta, South China Sea, Yellow River Estuary)
 857 and Japan (Tokyo Bay). *Journal of Hazardous Materials*, 371, 288-294.
 858 doi:<https://doi.org/10.1016/j.jhazmat.2019.03.029>
- 859 Li, J., Xie, Z., Mi, W., Lai, S., Tian, C., Emeis, K. C., et al. (2017). Organophosphate
 860 esters in air, snow, and seawater in the North Atlantic and the Arctic. *Environmental*
 861 *Science & Technology*, 51(12), 6887-6896.
 862 doi:<https://doi.org/10.1021/acs.est.7b01289>
- 863 Lian, M., Lin, C., Wu, T., Xin, M., Gu, X., Lu, S., et al. (2021). Occurrence,
 864 spatiotemporal distribution, and ecological risks of organophosphate esters in the
 865 water of the Yellow River to the Laizhou Bay, Bohai Sea. *The Science of the total*
 866 *environment*, 787, 147528-147528.
 867 doi:<https://doi.org/10.1016/j.scitotenv.2021.147528>
- 868 Pantelaki, I., & Voutsas, D. (2021). Organophosphate esters in inland and coastal waters in
 869 northern Greece. *Science of the Total Environment*, 800, 149544.
 870 doi:<https://doi.org/10.1016/j.scitotenv.2021.149544>
- 871 Schmidt, N., Fauvelle, V., Ody, A., Castro-Jiménez, J., Jouanno, J., Changeux, T., et al.
 872 (2019). The Amazon River: A major source of organic plastic additives to the
 873 tropical North Atlantic? *Environmental Science & Technology*, 53(13), 7513-7521.
 874 doi:<https://doi.org/10.1021/acs.est.9b01585>
- 875 Shi, Y., Zhang, Y., Du, Y., Kong, D., Wu, Q., Hong, Y., et al. (2020). Occurrence,
 876 composition and biological risk of organophosphate esters (OPEs) in water of the

- 877 Pearl River Estuary, South China. *Environmental Science and Pollution Research*,
878 27(13), 14852-14862. doi:<https://doi.org/10.1007/s11356-020-08001-1>
- 879 Sutton, R., Chen, D., Sun, J., Greig, D. J., & Wu, Y. (2019). Characterization of
880 brominated, chlorinated, and phosphate flame retardants in San Francisco Bay, an
881 urban estuary. *Science of The Total Environment*, 652, 212-223.
882 doi:<https://doi.org/10.1016/j.scitotenv.2018.10.096>
- 883 Verbruggen, E. M. J., Rila, J. P., Traas, T. P., Posthuma-Doodeman, C. J. A. M., &
884 Posthumus, R. (2005), Environmental risk limits for several phosphate esters, with
885 possible application as flame retardant (*Rep. 601501024*). Bilthoven: Netherlands
886 National Institute for Public Health and the Environment.
- 887 Xiao, K., Lu, Z., Yang, C., Zhao, S., Zheng, H., Gao, Y., et al. (2021). Occurrence,
888 distribution and risk assessment of organophosphate ester flame retardants and
889 plasticizers in surface seawater of the West Pacific. *Marine Pollution Bulletin*, 170.
890 doi:<https://doi.org/10.1016/j.marpolbul.2021.112691>
- 891 Zheng, H., Cai, M., Yang, C., Gao, Y., Chen, Z., & Liu, Y. (2022). Terrigenous export and
892 ocean currents' diffusion of organophosphorus flame retardants along China's
893 adjacent seas. *Environmental Pollution*, 299, 118873.
894 doi:<https://doi.org/10.1016/j.envpol.2022.118873>
- 895 Zhong, M., Tang, J., Guo, X., Guo, C., Li, F., & Wu, H. (2020). Occurrence and spatial
896 distribution of organophosphorus flame retardants and plasticizers in the Bohai,
897 Yellow and East China seas. *Science of the Total Environment*, 741.
898 doi:<https://doi.org/10.1016/j.scitotenv.2020.140434>